Coherent backscattering of elastic waves: Specific role of source, polarization, and near field

B. A. van Tiggelen[a)]
CNRS/Laboratoire de Physique et Modélisation des Milieux Condensés, Université Joseph Fourier, Maison des Magistères, B.P. 166, 38042 Grenoble Cedex 09, France

L. Margerin and M. Campillo
Laboratoire de Géophysique Interne et Tectonophysique, Observatoire de Grenoble, Université Joseph Fourier, B.P. 53, 38041 Grenoble Cedex, France

(Received 20 July 2000; revised 10 March 2001; accepted 2 May 2001)

Calculation of coherent backscattering of elastic waves in an infinite isotropic random medium is presented. Despite the simplicity of this geometry, this calculation highlights several specific aspects for seismic detection: near field detection, polarization, and the symmetry of the source. Line profiles and enhancement factors are seen to be time independent and are calculated for kinetic, shear, and compressional energy. © *2001 Acoustical Society of America.*
[DOI: 10.1121/1.1388017]

PACS numbers: 43.20.Gp, 43.20.Bi, 91.30.Dk [DEC]

I. INTRODUCTION

Coherent or enhanced backscattering finds its origin in interference effects in multiple scattering of waves. Basic is the reciprocity principle which states that partial waves propagating in opposite directions interfere constructively at the source from which they originate, no matter how complex the wave path.[1] These ideas were originally developed in condensed matter,[2] where such constructive interferences give rise to the so-called ''weak localization'' corrections to the electrical conductance. In the beginning of the 1980s, coherent backscattering of light was observed independently by different groups.[3,4] Since then, a lot of theoretical and experimental efforts have been undertaken to understand this novel effect in detail, such as the role of an external magnetic field, which breaks time-reversal symmetry,[5,6] chirality,[6] line shape,[7] enhancement factor,[8] stimulated emission,[9] and Raman scattering.[10] More recently, time-dependent enhanced backscattering was reported for acoustic waves.[11]

Wave scattering is also of interest in seismic applications. Since the pioneering work of Aki[12] and Aki and Chouet[13] three decades ago, seismic coda is interpreted as elastic waves scattered from randomly distributed inhomogeneities in the Earth's crust. The seismic coda refers to the exponential time tail observed in the seismograms of local earthquakes in the frequency band 1–10 Hz. Whereas early work[12,14,15] tried to model the coda as singly scattered waves in a uniform space, recent numerical studies suggested the importance of multiple scattering.[16–19] In the above-mentioned frequency band the mean free path of the elastic waves is estimated to be $l \approx 20-70$ km.[20] Given a typical velocity of 3.5 km/s the mean free time between two scattering events would be 20 s maximum. This time scale supports the view that seismic coda, which often lasts for more than 200 s, is a genuine multiple scattering phenomenon. A detailed theoretical study of enhanced backscattering of elastic waves is necessary to facilitate its observation in seismic data.

The presence of three polarizations and two different speeds makes any multiple scattering problem in elasticity considerably more complicated than in electromagnetism. The technical aspects have been studied in great detail by Weaver,[21] Turner and Weaver,[22] and Papanicolaou *et al.*[23] Seismic observations are characterized by a number of additional specific aspects, and the present work aims to address some of them.

First, seismic measurements are always carried out in the near field, i.e., near or in the scattering medium, in contrast to previous far-field scattering studies with light and acoustic waves. Our first study,[24] carried out for acoustic waves, has revealed that observation of enhanced backscattering of seismic waves requires detection within approximately one elastic wavelength (typically 100 m to 1 km) from the seismic source, making it a genuine near field effect. This characteristic distance is quite different from the one in the far field, where it equals the much longer mean free path.[8,11] The line shape of enhanced backscattering can be defined as the ratio of enhancement near the source, normalized to the energy measured far way. Studies with light[25] and acoustic waves[11] in the far field showed this ratio to be a function of time. In the near field, a *stable* line shape was predicted at times longer than the mean free time, with a maximal enhancement factor equal to 2 at the source and a typical distance of one wavelength for the enhancement to vanish. The present work investigates the precise line profile for enhanced backscattering in an infinite medium, using the full theory of elasticity. The complex role of the nearby free surface, which induces mode conversions, is left to future work.

The second specific aspect is that seismic sources are known to be highly polarized. The role of polarization has been shown to be crucial in optical studies, since the reciprocity principle applies only when detector and source have the same polarization.[1,7] The explosions have a diagonal seis-

a)Electronic mail: tiggelen@belledonne.polycnrs-gre.fr

mic moment tensor, releasing compressional energy only. Being relatively under control, they seem good candidates for enhanced backscattering studies. Unfortunately, because of the low shear velocity, multiple scattering rapidly converts most elastic energy into shear excitations,[26] and an observation of enhanced backscattering with explosions seems *a priori* hopeless. On the other hand, earthquakes are often modeled by a dislocation, with a traceless, symmetric seismic moment tensor, characteristic of a source involving a double couple.[27] The diagonal elements of the seismic moment tensor of an earthquake, corresponding to volume changes, are estimated to be small, typically of the order of 2%. This particular symmetry of the source has never been discussed in the context of multiple scattering and enhanced backscattering.

Our study is closely related to a recent study by De Rosny, Tourin, and Fink[28] and Weaver and Lobkis,[29] which involve the enhanced backscattering effect of elastic waves in a reverberant cavity. The main difference is that in reverberant cavities the mixing of the waves is caused by the chaotic nature of their boundaries, and not by elastic scatterers inside. Second, in a finite cavity, an additional characteristic time exists, the Heisenberg time, beyond which the enhanced backscattering factor changes from 2 to 3. This Heisenberg time is infinite for an infinite random medium. In this paper we show that the enhancement factor for coherent backscattering in an infinite elastic medium is necessarily less than or equal to 2. Sometimes the enhancement can be so small that observation is very unlikely, since the effect is easily overwhelmed by measurement errors. The study by De Rosny *et al.*[28] of two-dimensional enhanced backscattering of elastic waves in a chaotic silicon wafer has revealed a very unconventional line shape, vanishing exactly at the source and with two maxima at roughly one wavelength from the source. This line profile was explained by the *dipolar* nature of the source.[30]

II. SOURCE: EXPLOSIONS AND DISLOCATIONS

In general, seismic sources can be described by a force field $f_i(\mathbf{r},t)$ localized in space and time. This force field contains a wide range of frequencies ω and we shall represent it by its Fourier transform $f_i(\mathbf{r},\omega)$. For sources small compared to the elastic wavelength, the following multipole expansion applies:

$$f_i(\mathbf{r},\omega)=F_i(\omega)\,\delta(\mathbf{r})-M_{in}(\omega)\,\partial_n\delta(\mathbf{r})+\cdots. \tag{1}$$

The net force F_i and the seismic moment tensor M_{in} are defined by

$$F_i(\omega)\equiv\int d\mathbf{r}\, f_i(\mathbf{r},\omega),\quad M_{in}(\omega)\equiv\int d\mathbf{r}\, r_n f_i(\mathbf{r},\omega), \tag{2}$$

where the integral is carried out over the whole source. The process initiating the source has no external perturbations, so that the net force F_i and the net couple $M_{ij}-M_{ji}$ $(i\neq j)$ must vanish. Thus, the seismic moment tensor must be *symmetric*. The diagonal elements M_{ii} induce no couple but create compressional deformations, typical of explosions. An ideal, isotropic explosion can be characterized by the seismic moment tensor $M_{ij}=M\delta_{ij}$. Earthquakes are believed to be dislocations with very small volume changes. This reduces the model to one with two compensating dipolar couples, hence the name ''double couple.'' Only vulcano eruptions are examples of seismic sources for which a net force $F_i(\omega)$ is believed to exist.

The force field $f_j(\mathbf{r},\omega)$ acts as the source term in the elastic wave equation for the displacement vector $u_i(\mathbf{r})$, whose Green's tensor is denoted by G_{ij}.[27] From Eq. (1), it follows immediately that the elastic wave released at the source is

$$u_i(\omega,\mathbf{r})=M_{nj}(\omega)\,\partial_n G_{ij}(\omega,\mathbf{r}). \tag{3}$$

This source field will be used as a starting point for coherent backscattering calculations. In an isotropic homogeneous elastic medium the elastic Green's tensor is[27]

$$\begin{aligned}G_{ij}(\omega,\mathbf{r})=&-\frac{3\hat{r}_i\hat{r}_j-\delta_{ij}}{4\pi r^3}\int_{r/\alpha}^{r/\beta}dy\, y\exp(i\omega y)\\&-\frac{\hat{r}_i\hat{r}_j}{4\pi\alpha^2 r}\exp(i\omega r/\alpha)\\&+\frac{\hat{r}_i\hat{r}_j-\delta_{ij}}{4\pi\beta^2 r}\exp(i\omega r/\beta).\end{aligned} \tag{4}$$

The inequality $\alpha\neq\beta$ of the two elastic velocities gives rise to the first near-field term.

III. COHERENT BACKSCATTERING IN THE NEAR FIELD

In the following we assume that multiple scattering does not affect the frequency ω, and often drop the frequency label. The basic observable used in radiative transfer of elastic waves is the correlation function of two elastic displacement vectors $\langle u_i(\mathbf{r}-\frac{1}{2}\mathbf{x},t)u_j^*(\mathbf{r}+\frac{1}{2}\mathbf{x},t')\rangle$ at two different positions and for two different times. One time label can be transformed away in favor of a central carrier frequency ω. The time label that remains describes the time evolution of the ''slowly varying'' envelope of the pulse, which is much slower than the harmonic cycle.

The kernel $L_{ij\to kl}(\mathbf{r}_1,\mathbf{r}_2\to\mathbf{r}_3,\mathbf{r}_4,t)$ describes the transfer of the displacement correlation function from source (displacement indices i, j and positions $\mathbf{r}_1$, $\mathbf{r}_2$) to detector (displacement indices k, l and positions $\mathbf{r}_3$, $\mathbf{r}_4$). Standard radiative transfer theory neglects all interference effects in the vertex L and assumes that the field $\mathbf{u}$ and its complex conjugate $\mathbf{u}^*$ travel along exactly the same paths, so that their phase difference cancels. This leads to the diagrammatic ''ladder'' representation of L shown in Fig. 1(a). The solid lines denote a Green's tensor that quantifies the radiation from one scatterer to the next, displayed as crosses. We emphasize that the diagram denotes the propagation of the displacement Stokes tensor $\langle u_j u_j^*\rangle$. Both the release of energy by the source and the measurement carried out at the detector can be described by some linear operation of this Stokes tensor which will be specified in the following.

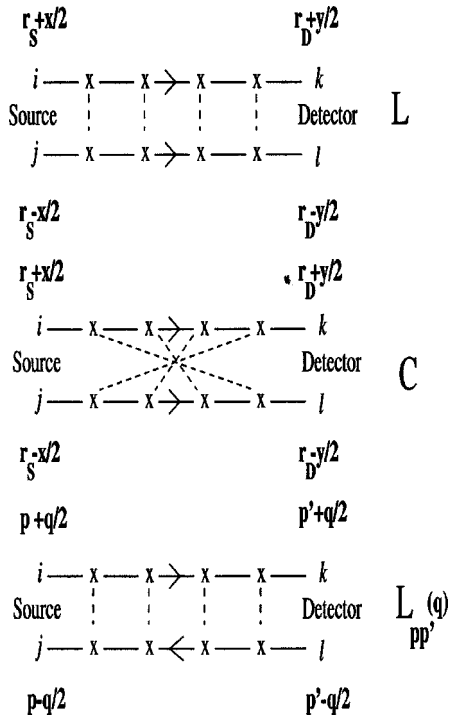

FIG. 1. Diagrammatic representations of incoherent propagation of elastic displacements (top), and interference between time-reversed wave (middle). Crosses denote scatterers, a solid line denotes the Green's function of the elastic wave equation. Dashed lines connect identical scatterers. The bottom diagram denotes the incoherent propagation in Fourier space.

The basic physics of the coherent backscattering is the interference between time reversed paths. If the sequence of scattering events, which starts at the source and ends at the detector is time reversed, the diagram 1(b) is obtained, representing the vertex C. The reciprocity principle gives a very simple relation between both vertices,[1]

$$C_{ijkl}(t,\mathbf{r}_1,\mathbf{r}_2\rightarrow\mathbf{r}_3,\mathbf{r}_4)=L_{ilkj}(t,\mathbf{r}_1,\mathbf{r}_4\rightarrow\mathbf{r}_3,\mathbf{r}_2), \tag{5}$$

i.e., polarization labels and positions of bottom line simply interchange.

The interference contribution C is not contained in classical radiative transfer, but will significantly modify the energy coming back to the source. This can best be seen for the simplified case of a measurement of $\langle|u_k(\mathbf{r}_d)|^2\rangle$, which is proportional to the average kinetic elastic energy at the detector, and a genuine monopole source $f_i(\omega)\delta(\mathbf{r}-\mathbf{r}_s)$. The last property means that the source emits the wave field $\mathbf{G}(\omega,\mathbf{r}-\mathbf{r}_s)\cdot\mathbf{f}(\omega)$ and not the one described by Eq. (3). In that case, L_{iikk} and C_{iikk} correspond *exactly* to the observation. Equation (5) implies

$$C_{iikk}(t,\mathbf{r}_s,\mathbf{r}_s\rightarrow\mathbf{r}_d,\mathbf{r}_d)=L_{ikki}(t,\mathbf{r}_s,\mathbf{r}_d\rightarrow\mathbf{r}_d,\mathbf{r}_s). \tag{6}$$

This relation means that $C=L$ at all times for detection at the source ($\mathbf{r}_s=\mathbf{r}_d$) provided that the displacement component is measured along the polarization of the source ($i=k$). Since C may be expected to vanish away from the source, we would find a local enhancement of kinetic energy of *exactly* a factor of 2. In addition, at very long times we may expect incoherent radiation to be completely depolarized, $L_{ikki}(t)\sim\delta_{ik}$. This means that the interference C vanishes for any component orthogonal to the polarization of the source. This would be very useful to determining the polarization of a seismic source with waves in the regime of seismic coda, where multiple scattering is believed to occur.

A. Coherent backscattering near a seismic source

The above-mentioned arguments have been shown to apply to experiments carried out in the far field for both light[3] and acoustic waves,[11] where the factor of 2 was confirmed. For light also the absence of intensity enhancement in the orthogonal polarization channel has been established. The seismic situation is more complicated in view of the aspects of the source and the near field detection.

We restrict our analysis to elastic wave diffusion in an *infinite* medium, whose translational symmetry facilitates a study of the vertex L in the Fourier space. Evidently, the study with plane waves is a natural choice in optics.[1,6] The convention is shown in Fig. 1(c), introducing the four momenta $\mathbf{p}\pm\frac{1}{2}\mathbf{q}$ and $\mathbf{p}'\pm\frac{1}{2}\mathbf{q}$. Note the bottom line that travels in the opposite direction since it represents the complex conjugate of the displacement vector, so that the law of momentum conservation is obeyed, as required by translational symmetry. At times longer than the mean free time, the four-rank tensor L is dominated by its second-rank eigenfunction S_{ij} that corresponds to the eigenvalue closest to zero. This eigenvalue is given by $-Dq^2+1/\tau_a$ with D the diffusion constant and τ_a allowing for some small dissipation. (See Refs. 1 and 31 for more technical detail.) We get for the vertex L in the momentum representation,

$$L_{ijkl,\mathbf{pp}'}(t,\mathbf{q})\rightarrow e^{-Dq^2t-t/\tau_a}S_{ij}(\mathbf{p},\mathbf{q})S^*_{lk}(\mathbf{p}',\mathbf{q}). \tag{7}$$

The symmetric form of the vertex, which is invariant with respect to interchanging the source and the detector, is a manifestation of the reciprocity principle. The tensor $S_{ij}(\mathbf{p},\mathbf{q})$ determines the polarization of the diffuse field propagating in the direction $\mathbf{p}$, and fixes the elastic Stokes parameters completely.[22,23] It is given by[31]

$$S_{ij}(\mathbf{p},\mathbf{q})=G_{ij}(\mathbf{p}+\tfrac{1}{2}\mathbf{q})-G^*_{ji}(\mathbf{p}-\tfrac{1}{2}\mathbf{q}) \tag{8}$$

in terms of the elastic Green's tensor defined in Eq. (4), the asterisk denoting the complex conjugate.[32]

For our purposes we need the real space formulation, which can be obtained by the Fourier transformation,

$$\begin{aligned}
&L_{ijkl}(t,\mathbf{r}_1,\mathbf{r}_2\rightarrow\mathbf{r}_3,\mathbf{r}_4)\\
&\quad=\int\frac{d\mathbf{p}}{(2\pi)^3}\int\frac{d\mathbf{p}'}{(2\pi)^3}\int\frac{d\mathbf{q}}{(2\pi)^3}\\
&\qquad\times e^{i(\mathbf{p}+\mathbf{q}/2)\cdot\mathbf{r}_1}e^{-i(\mathbf{p}-\mathbf{q}/2)\cdot\mathbf{r}_2}e^{-i(\mathbf{p}'+\mathbf{q}/2)\cdot\mathbf{r}_3}\\
&\qquad\times e^{i(\mathbf{p}'-\mathbf{q}/2)\cdot\mathbf{r}_4}e^{-Dq^2t-t/\tau_a}S_{ij}(\mathbf{p},\mathbf{q})S^*_{lk}(\mathbf{p}',\mathbf{q})\\
&\quad\sim\frac{e^{-t/\tau_a}}{(Dt)^{3/2}}\int\frac{d\mathbf{p}}{(2\pi)^3}\int\frac{d\mathbf{p}'}{(2\pi)^3}e^{i\mathbf{p}\cdot\mathbf{r}_1}\\
&\qquad\times e^{-i\mathbf{p}\cdot\mathbf{r}_2}e^{-i\mathbf{p}'\cdot\mathbf{r}_3}e^{i\mathbf{p}'\cdot\mathbf{r}_4}\,\mathrm{Im}\,G_{ij}(\mathbf{p})\,\mathrm{Im}\,G_{lk}(\mathbf{p}')\\
&\quad=\frac{e^{-t/\tau_a}}{(Dt)^{3/2}}\,\mathrm{Im}\,G_{ij}(\mathbf{r}_1-\mathbf{r}_2)\,\mathrm{Im}\,G_{lk}(\mathbf{r}_4-\mathbf{r}_3).
\end{aligned} \tag{9}$$

The approximation carried out in the second line holds for large lapse times, where typically $q \approx 0$. The factor $e^{-t/\eta_a}/(Dt)^{3/2}$ is reminiscent of a diffusion process in three dimensions. In the rest of this paper we neglect absorption. The vertex C can be easily constructed using the reciprocity relation (5),

$$C_{ijkl}(t,\mathbf{r}_1,\mathbf{r}_2 \rightarrow \mathbf{r}_3,\mathbf{r}_4) = \frac{1}{(Dt)^{3/2}} \operatorname{Im} G_{il}(\mathbf{r}_1-\mathbf{r}_4) \operatorname{Im} G_{jk}(\mathbf{r}_2-\mathbf{r}_3). \tag{10}$$

This tensor describes the displacement correlation function $\langle u_k(\mathbf{r}_3) u_l^*(\mathbf{r}_4)\rangle$ which is due to constructive interference, for an arbitrary source. It is nonzero only near the source ($\mathbf{r}_1 \approx \mathbf{r}_4$ and $\mathbf{r}_3 \approx \mathbf{r}_2$). This analysis confirms the conclusion, which was reached previously for acoustic waves, that the line profile C/L around the source is *independent* of time.[24] The characteristic length in the line profile $\operatorname{Im} G_{il}(\mathbf{x})$ is typically the wavelength of compressional or shear waves, i.e., in the near field the phenomenon of coherent backscattering is diffraction limited. For a given distance x from the source, the relative enhancement factor C/L is highly dependent on frequency, typically proportional to $\sin^2(\omega x/\alpha)/x^2\omega^2$. This specific near-field feature may facilitate its observation.

In the following sections L_{kl} and C_{kl} are, respectively, the incoherent and coherent contribution to the displacement correlation function $\langle u_k u_l^*\rangle$ as measured at or near the source.

B. Enhancement of kinetic energy

Seismic studies address the three components of the displacement field $\mathbf{u}(t)$. Let us assume that the detection process produces the correlation functions $\langle u_k(\mathbf{r},t) u_l^*(\mathbf{r},t)\rangle$ between two displacement vectors at the same point. For $k=l$ this is the kinetic elastic energy density, proportional to $\omega^2\mathbf{u}^2$. For the source described in Eq. (3), incoherent and coherent contributions to $\langle u_k u_l^*\rangle$ at the detector may be obtained from Eqs. (9) and (10), respectively, by carrying out the spatial differentiation,

$$\begin{aligned} L_{kl}(\omega,\mathbf{r}_s,\mathbf{r}_d) &\sim \frac{-\omega^2}{(Dt)^{3/2}} \operatorname{Im} G_{kl}(\omega,\mathbf{0}) \\ &\quad \times M_{ni}(\omega) M_{mj}(\omega) \partial_m \partial_n \\ &\quad \times \operatorname{Im} G_{ij}(\omega,\mathbf{x}=0), \\ C_{kl}(\omega,\mathbf{r}_s,\mathbf{r}_d) &\sim \frac{\omega^2}{(Dt)^{3/2}} M_{mi}(\omega) M_{nj}(\omega) \\ &\quad \times \partial_m \operatorname{Im} G_{il}(\omega,\mathbf{x}) \partial_n \operatorname{Im} G_{jk}(\omega,\mathbf{x}). \end{aligned} \tag{11}$$

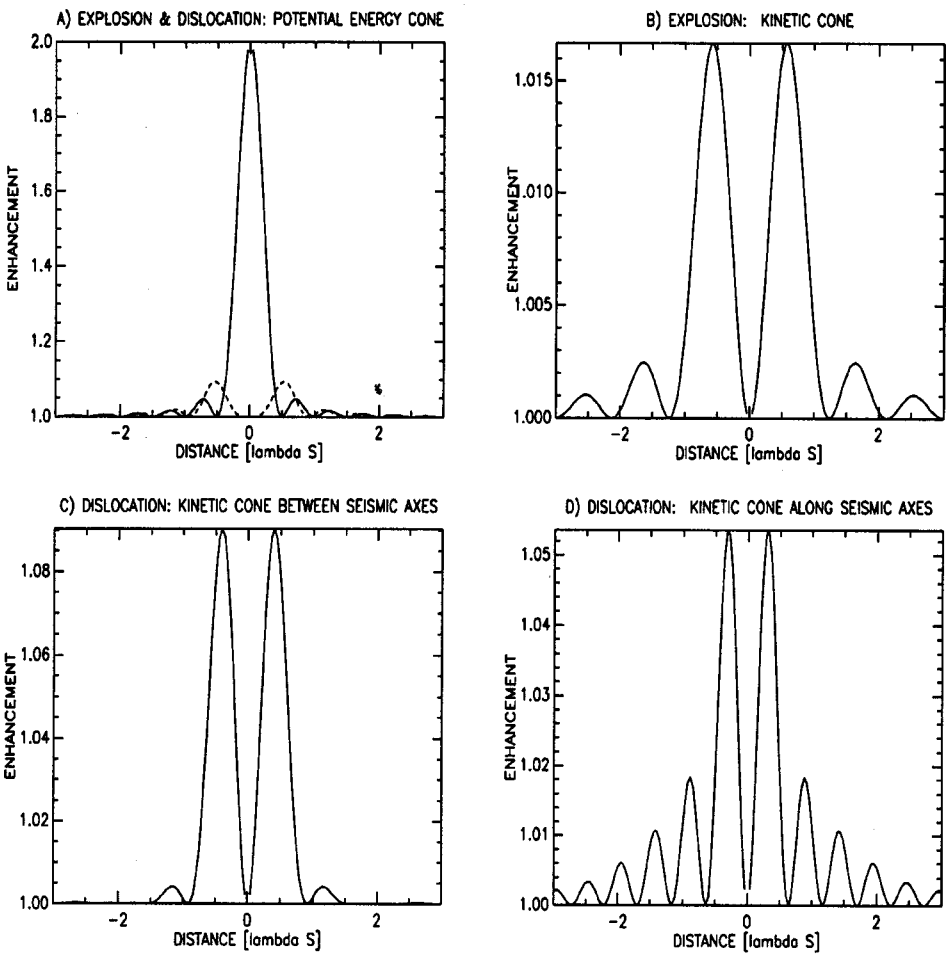

FIG. 2. Enhancement profiles as a function of the distance from the source, in units of the shear wave length, for an infinite Poissonian medium. (a) The enhancement of the potential energy for an explosion (solid) and a dislocation (dashed). (b) Enhancement profile for the kinetic energy near an explosion. (c) and (d) Enhancement profiles for the kinetic energy between and along the seismic axes of a dislocation source.

As usual, the implicit summation over the repeating indices is assumed, and $\mathbf{x}=\mathbf{r}_d-\mathbf{r}_s$ denotes this distance. The incoherent background L_{kl} is independent of the distance of the source. Explicitly, we have

$$L_{kl}(\omega,t)=\delta_{kl}\frac{\omega^6}{48\pi^2(Dt)^{3/2}}\left(\frac{1}{\alpha^3}+\frac{2}{\beta^3}\right)\left[\left(\frac{1}{\alpha^5}-\frac{1}{\beta^5}\right)\times\frac{2\,\mathrm{Tr}\,\mathbf{M}^2+(\mathrm{Tr}\,\mathbf{M})^2}{15}+\frac{1}{3\beta^5}\mathrm{Tr}\,\mathbf{M}^2\right]. \tag{12}$$

The factor δ_{kl} implies that the orthogonal displacements are decorrelated by high orders in multiple scattering. For $\alpha>\beta$, true for a Poissonian solid, the incoherent background is dominated by shear waves, that is the β terms in Eq. (12).

The coherent background C_{kl} decays as an oscillating power law away from the source. Somewhat surprisingly, we find that $C_{k=l}(\mathbf{x}=0)=0$, that is at the source we have a *destructive* interference. This is not a violation of the reciprocity principle, since the different operations performed by the source [this operation is specified in Eq. (3) and involves a spatial derivative] and the detector (the detector is supposed to measure the displacement itself, and thus no spatial derivative is involved) break their mutual symmetry.

We proceed by considering the coherent enhancement of kinetic energy cone in two special cases.

1. Explosion

An isotropic explosion is characterized by a seismic moment tensor $M_{ij}=M(\omega)\delta_{ij}$. Using Eq. (11) we find

$$C_{kl}(\omega,\mathbf{x},t)=\hat{r}_k\hat{r}_l\frac{M(\omega)^2\omega^6}{16\pi^2(Dt)^{3/2}\alpha^8}j_1^2\left(\frac{\omega x}{\alpha}\right),$$
$$L_{kl}(\omega,\mathbf{x},t)=\delta_{kl}\frac{M(\omega)^2\omega^6}{48\pi^2(Dt)^{3/2}\alpha^5}\left(\frac{1}{\alpha^3}+\frac{2}{\beta^3}\right). \tag{13}$$

The coherent profile vanishes at $x=0$, i.e., at the source, and has its first maxima on a shell at $x\approx\frac{1}{3}\lambda_P$ away from the source. Only radial, longitudinal P waves contribute to the coherent background whereas the incoherent background is dominated by shear waves. This lowers the maximal enhancement factor of the total kinetic energy to only $0.1(\beta/\alpha)^3\approx 0.017$. Figure 2(b) shows the line profile for the kinetic energy around an explosion. Therefore, an observation of enhanced backscattering of kinetic energy, with an explosion source, is rather unlikely; these measurements will be dominated by statistical fluctuations.

2. Dislocation

A dislocation source may be defined by a slip vector along the x axis and a plane normal to the z axis.[27] It offers a generally accepted model for an earthquake. Its seismic moment tensor is $M_{ij}=M(\omega)(\hat{x}_i\hat{y}_j+\hat{y}_i\hat{x}_j)$. The xyz frame defines the azimuthal angle ϕ in the nodal plane and the poloidal angle θ in the usual way. Starting with Eq. (11), a long but straightforward calculation gives C_{kk} and L_{kk} (summed over all components k) near the source, as

$$C_{kk}(\omega,\mathbf{x},t)=\frac{M(\omega)^2\omega^4\sin^2\theta}{16\pi^2(Dt)^{3/2}\beta^8}[S_1(\omega,x)^2\sin^2\theta\sin^2 2\phi+S_2(\omega,x)^2(1-\sin^2\theta\sin^2 2\phi)],$$
$$L_{kk}(\omega,\mathbf{x},t)=\frac{M(\omega)^2\omega^4}{16\pi^2(Dt)^{3/2}}\left(\frac{1}{\alpha^3}+\frac{2}{\beta^3}\right)\left(\frac{2}{15\alpha^5}+\frac{8}{15\beta^5}\right) \tag{14}$$

with the two line-shape functions,

$$S_1(\omega,x)=-\frac{9}{y_s^4}[y_s\cos y_s-\sin y_s-y_p\cos y_p+\sin y_p]+\frac{4}{y_s^2}\left(\frac{\beta}{\alpha}\right)^2\sin y_p-\frac{3}{y_s^2}\sin y_s-\frac{1}{y_s}\left(\frac{\beta}{\alpha}\right)^3\cos y_p,$$
$$S_2(\omega,x)=+\frac{6}{y_s^4}[y_s\cos y_s-\sin y_s-y_p\cos y_p+\sin y_p]-\frac{2}{y_s^2}\left(\frac{\beta}{\alpha}\right)^2\sin y_p+\frac{3}{y_s^2}\sin y_s-\frac{1}{y_s}\cos y_s, \tag{15}$$

given in terms of the dimensionless distances $y_s\equiv\omega x/\beta$ and $y_p\equiv\omega x/\alpha$.

Part of the double-couple structure of the source may be recognized from the angular dependence of the line profiles, which are different along and between the two seismic axes of the dislocation (i.e., the two axes in its nodal plane with respect to which the seismic moment tensor is diagonal), and vanish perpendicular ($\theta=0$) to the nodal plane. The two top figures in Fig. 3 show two different views of the enhancement of kinetic energy in the seismic plane ($\theta=\pi/2$). Four major maxima may be recognized between the seismic axes. Despite the fact that both coherent and incoherent radiation are dominated by shear waves, the enhancement factor still does not exceed 10%, and vanishes at the source [see Fig. 2(d)].

C. Enhancement of potential energy

The potential energy density of an elastic plane wave $\mathbf{u}$ in an infinite medium is proportional to $\alpha^2(\mathrm{div}\,\mathbf{u})^2+\beta^2(\mathrm{rot}\,\mathbf{u})^2$. The first term represents the energy of the longitudinal P waves and the second, of the transverse S waves. In this section we will calculate the coherent enhancement profiles of both terms.

1. Enhancement of compressional energy

The compressional energy is proportional to $\alpha^2(\mathrm{div}\,\mathbf{u})^2$. Its coherent enhancement near a source with the seismic moment tensor $M_{ij}(\omega)$ may be calculated from the vertex $C_{ijkl}(t,\mathbf{r}_1,\mathbf{r}_2\rightarrow\mathbf{r}_3,\mathbf{r}_4)$ given in Eq. (10), as follows:

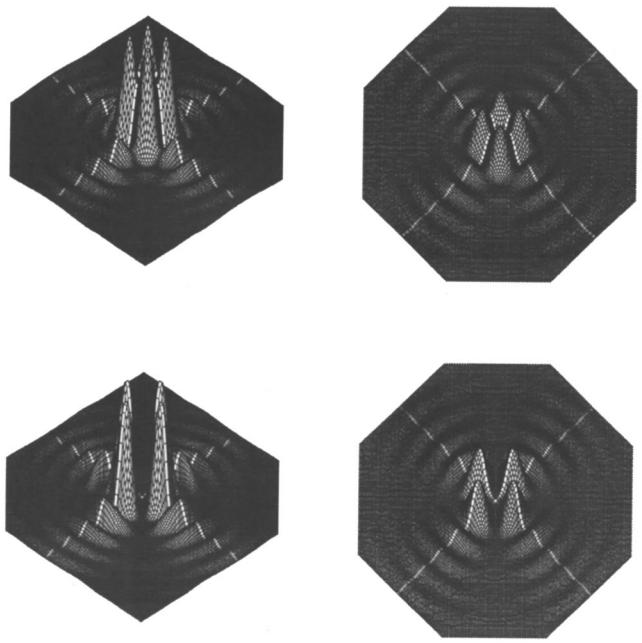

FIG. 3. Enhancement profiles of kinetic energy (top) and potential energy (bottom) in the seismic plane of a dislocation, from two different views. Distance is in units of the shear wavelength. The white axes denote the two seismic axes.

$$
\begin{aligned}
C_p &= \alpha^2 M_{ni}(\omega) M_{mj}(\omega) \partial_n^{(1)} \partial_m^{(2)} \partial_k^{(3)} \partial_l^{(4)} C_{ijkl}(t, \mathbf{r}_1, \mathbf{r}_2 \rightarrow \mathbf{r}_3, \mathbf{r}_4) \\
&= \frac{1}{(Dt)^{3/2}} M_{ni}(\omega) M_{mj}(\omega) \partial_n \partial_l \operatorname{Im} G_{il}(\omega, \mathbf{x}) \partial_m \partial_k \\
&\quad \times \operatorname{Im} G_{jk}(\omega, \mathbf{x}) \\
&= \frac{\omega^6}{16\pi^2 (Dt)^{3/2} \alpha^8} \left[j_2(y_p) \hat{\mathbf{x}} \cdot \mathbf{M}(\omega) \cdot \hat{\mathbf{x}} - \frac{j_1(y_p)}{y_p} \operatorname{Tr} \mathbf{M}(\omega) \right]^2 .
\end{aligned}
\tag{16}
$$

We recall that $y_p = \omega x / \alpha$. Similarly, the incoherent background L becomes

$$
\begin{aligned}
L_p(\omega, \mathbf{x}, t) = \frac{\omega^6}{16\pi^2 (Dt)^{3/2} \alpha^3} &\left[\left(\frac{1}{\alpha^5} - \frac{1}{\beta^5} \right) \right. \\
&\left. \times \frac{2 \operatorname{Tr} \mathbf{M}^2 + (\operatorname{Tr} \mathbf{M})^2}{15} + \frac{1}{3\beta^5} \operatorname{Tr} \mathbf{M}^2 \right].
\end{aligned}
\tag{17}
$$

For an isotropic explosion $M_{ij} = M(\omega) \delta_{ij}$ the enhancement ratio simplifies to

$$
\frac{C_p}{L_P} = j_0(y_p)^2 . \tag{18}
$$

This result is exactly the same as for an acoustic medium and a monopole source,[24] including the factor of 2 enhancement over the background. When measuring the compressional energy, the symmetry between the explosion source and detector is restored, so that the reciprocity principle applies again [see Fig. 2(a)].

For a dislocation source $\operatorname{Tr} \mathbf{M} = 0$ the enhancement of compressional energy becomes

$$
\frac{C_P}{L_P} \approx \frac{15}{16} \left(\frac{\beta}{\alpha} \right)^5 \sin^4 \theta \sin^2 2\phi j_2(y_p)^2 , \tag{19}
$$

where the azimuthal angle ϕ is defined in the seismic plane. The operation of measuring the compressional energy (i.e., $(\operatorname{div} \mathbf{u})^2$) yields a very small value when applied to the double-couple source. This is due to the fact that the dislocation sources release most of their energy as shear waves. Hence, the source and detector are highly "orthogonal" (in a sense that will be made explicit in Sec. IV) so that the enhancement vanishes rapidly (as x^4) near the source. The small factor $(\beta/\alpha)^5$ in Eq. (19) expresses the efficient $P-S$ mode conversion, which seriously hampers the enhancement of compressional energy near a dislocation source.

2. Enhancement of shear energy

The operation of measuring the shear energy is $\beta^2 \epsilon_{ijk} \epsilon_{inl} \partial_j u_k \partial_n u_l^*$, with ϵ_{ijk} the antisymmetric Levi-Cevitta tensor. Together with the operation carried out by the source, coherent and incoherent contributions to the shear energy at the detector become, respectively,

$$
\begin{aligned}
C_S &= \beta^2 M_{ni}(\omega) M_{mj}(\omega) \epsilon_{pqk} \epsilon_{prl} \partial_q^{(3)} \partial_r^{(4)} \partial_n^{(1)} \partial_m^{(2)} \\
&\quad \times C_{ijkl}(t, \mathbf{r}_1, \mathbf{r}_2 \rightarrow \mathbf{r}_3, \mathbf{r}_4) \\
&= \frac{\omega^6}{16\pi^2 (Dt)^{3/2} \beta^8} j_2(y_s)^2 |\hat{\mathbf{x}} \times [\mathbf{M}(\omega) \cdot \hat{\mathbf{x}}]|^2 , \\
L_S &= \frac{\omega^6}{8\pi^2 (Dt)^{3/2} \beta^3} \left[\left(\frac{1}{\alpha^5} - \frac{1}{\beta^5} \right) \frac{2 \operatorname{Tr} \mathbf{M}^2 + (\operatorname{Tr} \mathbf{M})^2}{15} \right. \\
&\quad \left. + \frac{1}{3\beta^5} \operatorname{Tr} \mathbf{M}^2 \right].
\end{aligned}
\tag{20}
$$

Not unexpectedly for an explosion the coherent enhancement vanishes entirely. For a dislocation source it vanishes only near the source (as x^4). The enhancement of shear energy does not suffer from mode conversions but is only 0.09 at the first maximum located at $1/2\lambda_s$ on the seismic axis [see Fig. 2(a)]. In Fig. 3 (bottom) we display the enhancement factor of the total potential energy $S+P$ in the seismic plane which, in a Poissonian elastic medium, is largely dominated by the shear energy.

IV. RECOVERING THE FACTOR OF 2

In most cases that we have studied, the enhancement factor vanishes exactly at the source. Our explanation is that the operation carried out at the detector has a symmetry which is different to the source.

To clarify this point, we investigate if there exists a measurement of the type $N_{nj} \partial_n u_j$ that restores the factor of 2 familiar from the optical and acoustic studies. In view of Eq. (3), the choice of $\mathbf{N} = \mathbf{M}$, i.e., an operation equal to the seismic moment tensor of the source, seems to be a good candidate, since it restores the symmetry between source and detector. The second point that we have to establish is uniqueness of this choice.

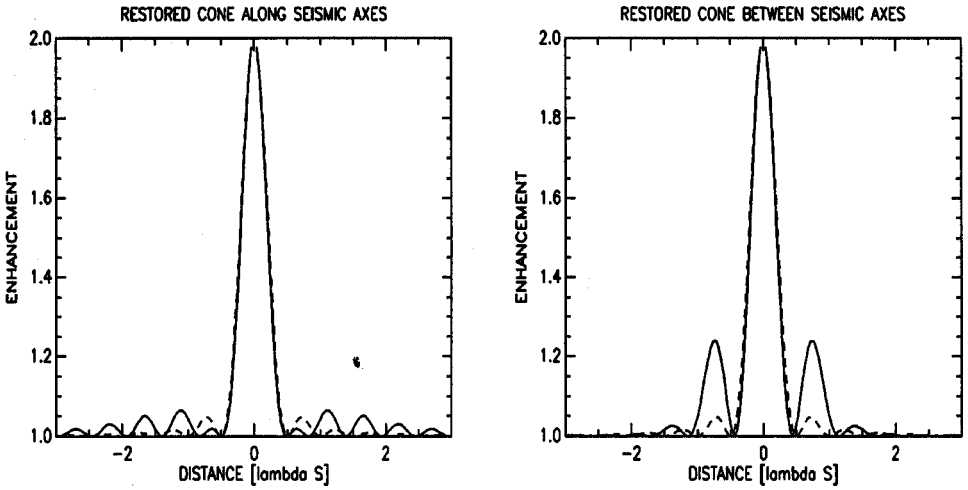

FIG. 4. Restoration of enhanced backscattering by carrying out exactly the same operation at the detector as at the dislocation source. Dashed line denotes the line profile for an acoustic source in an infinite medium. Distance is in units of the shear wavelength.

Upon measuring $N_{nj}\partial_n u_j$, the coherent enhancement becomes

$$C = M_{ni}M_{mj}N_{pk}N_{ql}\partial_n^{(1)}\partial_m^{(2)}\partial_p^{(3)}\partial_q^{(4)}C_{ijkl}(t,\mathbf{r}_1,\mathbf{r}_2\rightarrow\mathbf{r}_3,\mathbf{r}_4)$$

$$= \frac{1}{(Dt)^{3/2}}\times(M_{ni}N_{ql}\partial_n\partial_q \operatorname{Im} G_{il}(\mathbf{x}))^2. \tag{21a}$$

For the incoherent background the same operation yields

$$L = \frac{1}{(Dt)^{3/2}} M_{ni}M_{mj}\partial_n\partial_m \operatorname{Im} G_{ij}(\mathbf{x}=0)$$

$$\times N_{pk}N_{ql}\partial_p\partial_q \operatorname{Im} G_{kl}(\mathbf{x}=0). \tag{21b}$$

From Eq. (21) we conclude that if $\mathbf{M}=\mathbf{N}$ then $C(\mathbf{x}=0)=L$. This confirms our conjecture that the enhancement factor is fully restored if the detector carries out exactly the same operation as the source. The uniqueness of this choice for a dislocation source among all possible choices of $\mathbf{N}$ with a vanishing trace may be readily demonstrated. Using the Green's tensor (4) for an homogeneous isotropic elastic medium and Eq. (21), the enhancement factor becomes

$$\frac{C(\mathbf{x}=0)}{L} = \frac{(\operatorname{Tr}\mathbf{M}\cdot\mathbf{N})^2}{\operatorname{Tr}\mathbf{M}^2\operatorname{Tr}\mathbf{N}^2}. \tag{22}$$

The Cauchy inequality implies that $C(\mathbf{0})/L \leqslant 1$, with the equality holding *if and only if* $\mathbf{M}=\mathbf{N}$. This conclusion allows us to recover the seismic moment tensor by optimizing the enhancement near the source. Equation (22) also shows explicitly that the orthogonality of operations at source and detector leads to vanishing enhancement at the source.

Our final task is to calculate the line profile corresponding to the ideal choice. The scalar function $M_{ni}M_{mj}\partial_n\partial_m G_{ij}(\mathbf{x})$ for a general seismic moment tensor is presented in the Appendix. In Fig. 4 we show the restored line profile for a dislocation source, and compare it to the enhancement factor (18) which has been calculated for an explosion. Near the source they look very similar, but the "restored" profile is still anisotropic, with four significant secondary maxima at $x=0.7\lambda_s$ in between the seismic axes of the nodal plane.

V. CONCLUSION

We have calculated the spatial line profiles of the coherent enhancement factors of various elastic energies near the source. We have emphasized the seismic aspects of this elastic problem, in particular the specificity of the near-field detection. The first consequence of the near-field detection is the typical decay distance of the enhancement, which equals the elastic wavelength(s) and not the mean free path, as for the far-field detection. Second, the near field has a huge impact on the precise line profiles of the different measurable elastic energies. The operation performed at the detector (measuring kinetic energy, potential energy, etc.) as well as the precise symmetry of the source al play a crucial role. We have shown that *one unique* operation carried out at the detector shows the maximal possible enhancement of two. The enhancement of kinetic and potential energy vanishes at the source and does not exceed 10%. It is also hampered by mode conversions in multiple scattering. Only for an explosion source and a measurement of compressional energy is an enhancement of two is expected.

ACKNOWLEDGMENTS

We thank Julien de Rosny, Nicolas Trégourès, Mathias Fink, and Renaud Hennino for helpful discussions.

APPENDIX: LINE PROFILE OF RESTORED ENHANCEMENT

The restored line profile is given by Eq. (21a), in which figures the scalar function $M_{ni}M_{nj}\partial_n\partial_m \operatorname{Im} G_{ij}(\mathbf{x})$, which we state here without derivation for the case of a pure dislocation that obeys $\operatorname{Tr}\mathbf{M}=0$. Using the notation $y_s=\omega x/\beta$, $y_p=\omega x/\alpha$, and $R=\alpha/\beta$,

$$
\begin{aligned}
&\frac{1}{\omega^3\alpha^5} M_{ni} M_{nj} \partial_n \partial_m \operatorname{Im} G_{ij}(\mathbf{x}) \\
&\quad = 3(10\hat{\mathbf{x}}\cdot\mathbf{M}^2\cdot\hat{\mathbf{x}} - 10(\hat{\mathbf{x}}\cdot\mathbf{M}\cdot\hat{\mathbf{x}})^2 - 2)\left(\frac{\cos y_p}{y_p^4} - R\frac{\cos y_s}{y_p^4} + \frac{\sin y_s - \sin y_p}{y_s^3}\right) \\
&\qquad - 3(2\hat{\mathbf{x}}\cdot\mathbf{M}^2\cdot\hat{\mathbf{x}} - 5(\hat{\mathbf{x}}\cdot\mathbf{M}\cdot\hat{\mathbf{x}})^2)\left[\sin y_p\left(\frac{5}{y_p^5} - \frac{1}{y_p^3}\right) - \sin y_s\left(\frac{5}{y_p^5} - \frac{R^2}{y_p^3}\right) - \frac{5}{y_p^4}\cos y_p + \frac{5R}{y_p^4}\cos y_s\right] \\
&\qquad + 2(6\hat{\mathbf{x}}\cdot\mathbf{M}^2\cdot\hat{\mathbf{x}} - 6(\hat{\mathbf{x}}\cdot\mathbf{M}\cdot\hat{\mathbf{x}})^2 - 1)\frac{\sin y_p}{y_p^3} - 2(\hat{\mathbf{x}}\cdot\mathbf{M}^2\cdot\hat{\mathbf{x}} - 3(\hat{\mathbf{x}}\cdot\mathbf{M}\cdot\hat{\mathbf{x}})^2)\left(\frac{\cos y_p}{y_p^2} - \frac{3\sin y_p}{y_p^3}\right) \\
&\qquad - 3(4\hat{\mathbf{x}}\cdot\mathbf{M}^2\cdot\hat{\mathbf{x}} - 4(\hat{\mathbf{x}}\cdot\mathbf{M}\cdot\hat{\mathbf{x}})^2 - 1)R^2\frac{\sin y_s}{y_p^3} + 3(\hat{\mathbf{x}}\cdot\mathbf{M}^2\cdot\hat{\mathbf{x}} - 2(\hat{\mathbf{x}}\cdot\mathbf{M}\cdot\hat{\mathbf{x}})^2)\left(R^3\frac{\cos y_s}{y_p^2} - 3R^2\frac{\sin y_s}{y_p^3}\right) \\
&\qquad + (2\hat{\mathbf{x}}\mathbf{M}^2\cdot\hat{\mathbf{x}} - 2(\hat{\mathbf{x}}\cdot\mathbf{M}\cdot\hat{\mathbf{x}})^2 - 1)R^3\frac{\cos y_s}{y_p^2}(\hat{\mathbf{x}}\cdot\mathbf{M}^2\cdot\hat{\mathbf{x}} - (\hat{\mathbf{x}}\cdot\mathbf{M}\cdot\hat{\mathbf{x}})^2)\left(R^4\frac{\sin y_s}{y_p} + 2R^3\frac{\cos y_s}{y_p^2} - 2\frac{\cos y_p}{y_p^2}\right) \\
&\qquad \times(\hat{\mathbf{x}}\cdot\mathbf{M}\cdot\hat{\mathbf{x}})^2\left(\frac{\sin y_p}{y_p} + 2\frac{\cos y_p}{y_p^2}\right). \qquad \text{(A1)}
\end{aligned}
$$

[1] B. A. van Tiggelen and R. Maynard, ''Reciprocity and Coherent Backscattering of Light,'' in *Wave Propagation in Complex Media*, edited by G. Papanicolaou (Springer, New York, 1998).

[2] B. L. Altschuler, A. G. Aronov, and B. Z. Spivak, ''The Aharonov–Bohm effect in disordered conductors,'' JETP Lett. **33**, 94–97 (1981); D. Yu. Sharvin, and Yu. V. Sharvin, ''Magnetic flux quantization in a cylindrical film,'' *ibid.* **34**, 272–275 (1981).

[3] Y. Kuga and A. Ishimaru, ''Retroreflection from a dense distribution of spherical particles,'' J. Opt. Soc. Am. A **1**, 831–835 (1984); M. P. van Albada and A. Lagendijk, ''Observation of weak localization of light in a random medium,'' Phys. Rev. Lett. **55**, 2692–2695 (1985); P. E. Wolf and G. Maret, ''Weak localization and coherent backscattering of photons in disordered media,'' *ibid.* **55**, 2696–2699 (1985); M. Kaveh, M. Rosenbluh, I. Edrei, and I. Freund, ''Weak localization and light scattering from disordered solids,'' *ibid.* **57**, 2049–2052 (1986).

[4] *New Aspects of Eletromagnetic and Acoustic Wave Diffusion*, edited by POAN Research Group [Springer-Tracts Mod. Phys. **144**, 17–21 (1998)].

[5] F. A. Erbacher, R. Lenke, and G. Maret, ''Multiple light scattering in magneto-optically active media,'' Europhys. Lett. **21**, 551–556 (1993); D. Lacoste and B. A. van Tiggelen, ''Coherent backscattering in a magnetic field,'' Phys. Rev. E **61**, 4556–4565 (2000).

[6] F. C. MacKintosh and S. John, ''Coherent backscattering of light in the presence of time-reversal noninvariant and parity nonconserving media,'' Phys. Rev. B **37**, 1884–1897 (1988).

[7] E. Akkermans, P. E. Wolf, and R. Maynard, ''Coherent backscattering of light by disordered media: Analysis of peak-line shape,'' Phys. Rev. Lett. **56**, 1471–1473 (1986).

[8] D. S. Wiersma, M. P. van Albada, B. A. van Tiggelen, and A. Lagendijk, ''Experimental evidence for the occurrence of recurrent scattering of light in diffusion,'' Phys. Rev. Lett. **74**, 4193–4196 (1995).

[9] D. S. Wiersma, M. P. van Albada, and A. Lagendijk, ''Coherent backscattering of light from amplifying random media,'' Phys. Rev. Lett. **75**, 1739–1742 (1995).

[10] G. Labeyrie, F. de Tomasi, J.-C. Bernard, C. A. Müller, C. Miniatura, and R. Kaiser, ''Coherent backscattering of light by cold atoms,'' Phys. Rev. Lett. **83**, 5266–5269 (1999).

[11] G. Bayer and T. Niederdränk, ''Weak localization of acoustic waves in strongly scattering media,'' Phys. Rev. Lett. **70**, 3884–3887 (1993); A. Tourin, Ph. Roux, A. Derode, B. A. van Tiggelen, and M. Fink, ''Time-dependent coherent backscattering of acoustic waves,'' *ibid.* **79**, 3637–3639 (1997); K. Sakai, K. Yamamoto, and K. Takagi, ''Observation of acoustic coherent backscattering,'' Phys. Rev. B **56**, 10930–10933 (1997).

[12] K. Aki, ''Analysis of the seismic coda of local earthquakes as scattered waves,'' J. Geophys. Res. **74**, 615–631 (1969).

[13] K. Aki and B. Chouet, ''Origin of coda waves, source, attenuation and scattering effects,'' J. Geophys. Res. **80**, 3322–3342 (1975).

[14] H. Sato and M. C. Fehler, *Seismic Wave Propagation and Scattering in the Heterogeneous Earth* (Springer, Heidelberg, 1995).

[15] M. Herraiz and A. F. Spinoza, ''Coda waves: A review,'' Pure Appl. Geophys. **125**, 499–577 (1987).

[16] I. R. Abubakirov and A. A. Gusev, ''Estimation of scattering properties of the lithosphere of Kamchatka, based on Monte-Carlo simulations of record envelopes of a near earthquake,'' Phys. Earth Planet Inter. **64**, 52–67 (1990).

[17] M. Hoshiba, ''Simulation of multiple scattered coda wave excitations based on the Energy Conservation Law,'' Phys. Earth Planet. Inter. **67**, 126–136 (1991).

[18] H. Sato, ''Multiple isotropic scattering model including P–S conversions for the seismogram envelope formation,'' Geophys. J. Int. **117**, 487–494 (1994).

[19] R. S. Wu and K. Aki, ''Multiple scattering and energy transfer of seismic waves: Separation of scattering effects from intrinsic attenuation,'' Pure Appl. Geophys. **128**, 49–80 (1988).

[20] L. Margerin, M. Campillo, N. M. Shapiro, and B. A. van Tiggelen, ''Residence time of diffuse waves in the crust as a physical interpretation of coda Q,'' Geophys. J. Int. **138**, 343–352 (1999).

[21] R. L. Weaver, ''Diffusivity of ultrasound in polycrystals,'' J. Mech. Phys. Solids **38**, 55–86 (1990).

[22] J. A. Turner and R. Weaver, ''Radiative transfer and multiple scattering of diffuse ultrasound in polycrystalline media,'' J. Acoust. Soc. Am. **96**, 3675–3683 (1994).

[23] G. C. Papanicolaou, L. V. Ryzhik, and J. B. Keller, ''Stability of the P-to-S energy ratio in the diffuse regime,'' Bull. Seismol. Soc. Am. **86**, 1107–1115 (1996).

[24] L. Margerin, M. Campillo, and B. A. van Tiggelen ''Coherent backscattering of acoustic waves in the near field,'' Geoph. J. Int. (submitted).

[25] R. Vreeker, M. P. van Albada, R. Sprik, and A. Lagendijk, ''Femto-second time-resolved measurements of weak localization of light,'' Phys. Lett. A **132**, 51–55 (1988).

[26] R. L. Weaver, ''On diffuse waves in solid media,'' J. Acoust. Soc. Am. **71**, 1608–1609 (1982).

[27] T. Lay and T. C. Wallace, *Modern Global Seismology* (Academic, San Diego, 1995).

[28] J. de Rosny, A. Tourin, and M. Fink, ''Coherent backscattering of an elastic wave in a chaotic cavity,'' Phys. Rev. Lett. **84**, 1693–1695 (2000).

[29] R. L. Weaver and O. I. Lobkis, ''Enhanced backscattering and modal echo of reverberant elastic waves,'' Phys. Rev. Lett. **84**, 4942–4945 (2000).

[30] J. de Rosny, ''Milieux Réverbérants et Réversibilité,'' Ph.D. thesis, University of Paris, 2000.

[31] P. Sheng, *Introduction of Wave Scattering, Localization and Mesoscopic Phenomena* (Academic, San Diego, 1995).

[32] A detailed analysis (see, e.g., Ref. 31) shows that this Green's function should be the one of the effective medium, in which the elastic waves have a finite mean free path l due to scattering. This notion is irrelevant in the near field, since the wavelengths are much smaller than the mean free path.